

## EXPERIMENTAL RESULTS ON DUAL-UEGO ACTIVE CATALYST CONTROL

Giovanni Fiengo\* Jessy W. Grizzle\*\* Jeffrey A. Cook\*\*\*

\* *School of Engineering, Università degli Studi del Sannio,  
Benevento, Italy. E-mail: gifiengo@unisannio.it.*

\*\* *Electrical Engineering and Computer Science Department,  
University of Michigan, Ann Arbor, MI 48109-2122, USA.  
E-mail: grizzle@umich.edu*

\*\*\* *Ford Research Laboratory, Dearborn, MI, USA. E-mail:  
jcook2@ford.com*

Abstract: This paper describes active control of an aftertreatment system for a spark ignition engine equipped with a three-way catalyst and pre- and post-catalyst oxygen sensors. The control objective is to maximize the simultaneous conversion efficiencies of oxides of nitrogen and unburned hydrocarbons. Linear exhaust gas oxygen sensors are used to measure pre- and post-catalyst air-fuel ratio. A series controller configuration is adopted. The upstream controller provides relatively rapid response to disturbances on the basis of the pre-catalyst measurement, while the downstream controller uses the pre- and post-catalyst air-fuel ratio measurements to compensate for the bias corrupting the pre-catalyst air-fuel ratio measurement. The control strategy is tested on a 5.4L engine and compared with an existing proprietary controller that is based on the more common switching-type air-fuel ratio sensors.

### 1. INTRODUCTION

Conventional automotive gasoline engines employ a three-way catalytic converter (TWC) to oxidize HC and CO emissions and reduce NO<sub>x</sub>. Traditionally, the control emphasis has been on  $A/F$  feedback using a heated, switching-type exhaust gas oxygen (HEGO) sensor located in the exhaust manifold upstream of the TWC to maintain the  $A/F$  near stoichiometry and achieve high simultaneous conversion efficiencies. Recent requirements for onboard diagnostics (OBD) have led to the placement of an additional HEGO sensor downstream of the TWC. This secondary sensor is often used to trim the control action of the primary sensor; see Shafai et al. (1996) for related work using HEGO sensors and Ammann et al. (2000); Vemuri (1999) for work using UEGO sensors.

The authors presented in Fiengo et al. (2002) an air-fuel ratio ( $A/F$ ) control strategy based on linear exhaust gas oxygen (UEGO) sensors that directly addressed the non-equilibrium effects in the exhaust gas which can result in a bias error in

the air-fuel ratio sensor upstream of the catalyst. The goal of the present paper is to present a simplification of the previously reported control strategy and to present experimental verification of its performance on a 5.4L V8-engine equipped with dual underbody TWCs.

### 2. SYSTEM

Figure 1 illustrates the system to be controlled. It consists of a Spark Ignition Internal Combustion Engine (SI-ICE) equipped with an underbody TWC. Universal oxygen (UEGO) sensors provide a measurement of the oxygen content in the feedgas (upstream of the TWC) and tailpipe (downstream of the TWC) exhaust gas, respectively. In the case of a V-engine, the above description applies to each independent bank. In the case that two TWCs are present on an individual bank, the downstream sensor may be placed between the two TWCs or downstream of both TWCs.

Importantly, feedgas and tailpipe  $A/F$  measurements are affected by different types of inaccuracy. Upstream of the catalyst, non-equilibrium effects in the exhaust gas result in a bias error in the sensor; see Shulman and Hamburg (1980); Colvin et al. (1982); Hamburg et al. (1983); Germann et al. (1995, 1996). This bias is due in part to incomplete catalysis of CO on the sensor substrate and in lesser part to NOx; an additional confounding factor is the large discrepancy in the diffusion rate of  $H_2$  with respect to other species present in the exhaust gas. Assuming thermodynamic equilibrium in the exhaust gas after the catalyst, the measurement disturbance at the tailpipe  $A/F$  sensor is considered to be zero mean white noise.

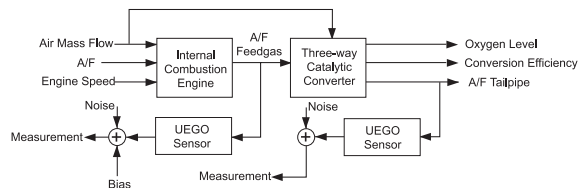


Fig. 1. Engine and Catalyst. Also shown are the upstream and downstream UEGO sensors.

### 3. CONTROL STRATEGY

The control strategy employed is a simplification of Fiengo et al. (2002). The controller is formed by two blocks connected in series<sup>1</sup>; see Figure 2. The objective of the first block, the *Fore Controller*, is to respond relatively quickly to  $A/F$  disturbances on the basis of measured feedgas oxygen level. As discussed in the previous section, feedgas oxygen measurement is corrupted by a systematic bias. The objective of the second block, the *Aft Controller*, is to adjust the setpoint of the fore-controller, on the basis of both  $A/F$  measurements, so that the TWC achieves simultaneously high conversion efficiencies for HC and NOx. The aft controller acts on a slower time scale commensurate with the longer measurement delay in the second sensor.

**Fore Controller:** The fore controller is realized by a switching-type PI controller. Measured  $A/F$  ratio is first compared to a reference value provided by the aft controller, resulting in an error signal of  $-1$  if measured  $A/F$  is lean of the reference and  $+1$  otherwise. The error signal is fed into a standard PI controller, with gains scheduled as a function of engine speed, so as to create a limit cycle with a (sensed) peak-to-peak amplitude of approximately  $0.2 A/F$  and period 1.5 seconds. Since typically a limiter is placed on the output of the controller, anti-windup is implemented.

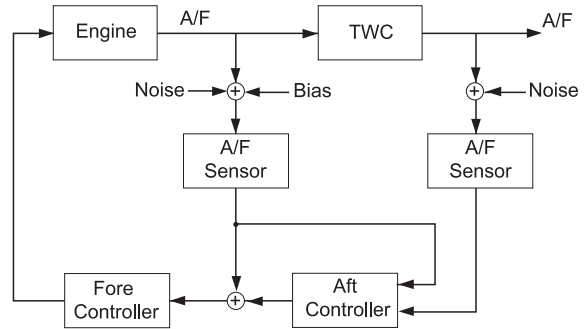


Fig. 2. Dual UEGO Fore-Aft Controller.

**Aft Controller:** The aft controller is composed of a bias estimator and a proportional term. The bias estimator uses upstream and downstream  $A/F$  measurements to correct the measurement of the upstream oxygen sensor. The proportional controller feeds back the post-catalyst UEGO sensor measurement and establishes the reference for the fore controller.

The bias estimator is based on the following observations. In the absence of a bias, the averages of the  $A/F$  in the feedgas and tailpipe should be the same whenever the feedgas signal remains constant for a period of time sufficiently long to fill an empty catalyst with oxygen or, conversely, to deplete a filled one. That is, if  $\lambda_{FG}$  is constant at a lean value,  $\lambda_{TP}$  will reach the same value when the catalyst is completely filled with oxygen. Conversely, if  $\lambda_{FG}$  is rich,  $\lambda_{TP}$  and  $\lambda_{FG}$  will be equal after the catalyst has been entirely depleted of oxygen. At stoichiometry,  $\lambda_{TP}$  equals  $\lambda_{FG}$ , independently of the oxygen state of the catalyst. Hence, in steady-state, the difference in the averaged values of the two measurements is due to the bias in the upstream sensor. The bias estimator is then subtracted from the output of the upstream UEGO sensor before it is used by the fore controller.

During transients, the bias estimator acts to indirectly control the level of oxygen stored in the catalyst. For example, suppose that  $\lambda_{FG}$  oscillates symmetrically around stoichiometry and that the catalyst is (nearly) depleted of oxygen. Then, the average of  $\lambda_{TP}$  will be slightly rich due to the fact that the TWC can only absorb oxygen when the feedgas is lean of stoichiometry. Consequently, the bias estimate will be larger than the actual bias, which has the same effect as increasing the setpoint of the fore controller to a leaner value; it follows that the  $A/F$  system is driven toward filling the catalyst with oxygen. Similar reasoning applies when the catalyst is (nearly) saturated with oxygen. Hence, as opposed to updating the bias estimate only in steady state as reported in Fiengo et al. (2002), here, the bias is updated continually. The estimated bias is also limited to a maximum and minimum range.

The proportional term is formed by subtracting the measured tailpipe  $A/F$  from the reference

<sup>1</sup> The standard feedforward control action based on measured or estimated mass air flow rate is not discussed; see Cook et al. (1996); Grizzle et al. (1994).

value and then multiplying by an “asymmetric” gain; that is, lean errors are corrected more aggressively than rich errors to avoid NO<sub>x</sub> breakthrough. The proportional term is then added to the reference value for tailpipe  $A/F$ , and provided to the fore-controller.

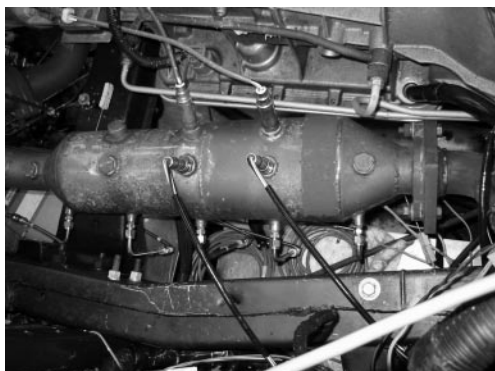


Fig. 3. Photograph of the TWC, Viewed From the Top. Feedgas is flowing from right to left. The emissions taps are visible at the bottom of the photograph, the UEGO sensors are in the middle, and the HEGO sensors are toward the top.

#### 4. EXPERIMENTAL FACILITY AND METHODOLOGY

The experiments were performed in a dynamometer test cell. A 5.4 L V8 engine and automatic transmission were connected to a motoring dynamometer. The dynamometer’s controller allowed speed-torque profiles approximating standard test cycles to be run, specifically, the warmed-up portion of the Federal test procedure (FTP) cycle. The FTP is comprised of three modes, or “bags” (referring to the fluropolymer bags in which emissions are stored for analysis). Bag 1 comprises a cold engine start and 505 second drive attaining a speed of about 57 mph. Bag 2 is a low speed, hot stabilized, drive cycle lasting 867 seconds. For bag 3, the engine is stopped for 10 minutes, after which a hot start is performed and the 505 second bag 1 is repeated. The experimental results described here are measured over bags 2 and 3.

The right side of the engine was used for evaluating the dual-UEGO  $A/F$  control strategy described in Section 3, along with a few variants. The exhaust system was modified to consist of a single underbody TWC, mounted approximately 30 cm downstream of the exhaust manifold; see Figure 3. A close-coupled catalyst for rapid light off upon cold start was not used. The underbody TWC consisted of four bricks of approximately equal volume but with different precious metal loadings. The oxygen storage capacities of bricks two and three were the same; brick one had 20% greater capacity and brick four had four times the capacity. The aftertreatment system had been aged for greater than 100 hours prior to testing. Thermocouples were inserted ahead of each brick

into the exhaust stream, and in the catalyst substrate 2.5 cm from the face of each brick. An emissions tap and two sensor bosses were installed between bricks one and two (referred to hereafter as the brick one location) and between bricks two and three (referred to hereafter as the brick two location); this allowed UEGO and HEGO data to be recorded simultaneously. Feedgas emissions and  $A/F$  were measured approximately 10 cm upstream of the catalyst. Emissions could be simultaneously recorded at two of the three points in the exhaust system, namely, feedgas, and one of brick one or brick two, for the purpose of determining conversion efficiencies of HC and NO<sub>x</sub> (CO was recorded but not analyzed).

The UEGO sensors were supplied with a nominal calibration curve. The calibration was refined in the test cell in the following manners. First of all, approximate linearity was verified through a standard  $A/F$  sweep over the range from 12  $A/F$  to 18  $A/F$ , where exhaust  $A/F$  was estimated from measured airmass flow rate and fuel pulse width. Stoichiometry was then more precisely estimated from catalyst conversion characteristics, namely, by correlating UEGO-sensor voltage readings to the point where the catalyst exhibited best simultaneous conversion of HC and NO<sub>x</sub>, as determined by the emissions benches. Finally, stoichiometry was also estimated through HEGO measurements. Using the HEGO sensor and a standard PI controller, an  $A/F$  limit cycle was established about stoichiometry. The UEGO sensor output was then sampled synchronously with the HEGO crossing stoichiometry, and averaged over ten crossings in each direction. The resulting estimated stoichiometric point for the UEGO agreed within  $0.03 \pm 0.002\%$  of the value estimated from the catalyst’s best conversion point.

The base software of the engine control unit was modified to allow the engine to be run with the standard—*baseline*—controller, or, to accept a replacement feedback signal generated externally to the engine control unit. More precisely, in the latter case, the feedforward portion of the onboard  $A/F$  control loop based on air charge estimation was retained, the onboard feedback loop was disabled, and the commanded fuel pulse width was multiplied by the value of the external signal. Hence when the external signal was one, the engine operated under nominal feedforward control, and by varying the external signal about one, commanded  $A/F$  could be varied rich or lean of the feedforward value, just as in a standard negative feedback loop. The external signal was generated in a real-time control prototyping system via the algorithm of Section 3.

The baseline controller implements a proprietary algorithm based on dual-HEGOs, one in the feedgas and one in the tailpipe. The algorithm was calibrated to function with the tailpipe HEGO at the brick two location.

## 5. EXPERIMENTAL RESULTS

The dual-UEGO control strategy of Section 3 was tested on the engine and exhaust system described in Section 4 over bags 2 and 3 of the FTP drive cycle. Figure 4 depicts measured engine speed over the cycle. The experiments were performed over a five week period in August-September 2002, concurrently with other work in the test cell. Cold start was not an objective of the testing plan, and hence multiple tests could be run in a single day (typically three to five, when the test cell was available). Since the catalyst would be in a “random” thermal state depending on the length of time since the previous test, the first 100 seconds of the cycle are neglected in the presentation of the results. The controller was operated with several variations: the tailpipe UEGO placed in brick one or brick two; bias estimation enabled always or only in steady state; and the aft controller with and without the proportional term. The baseline controller was always operated with the tailpipe  $A/F$  measurement at brick two. The setpoint of the dual-UEGO controller was selected to be stoichiometry, that is,  $\lambda = 1$ . In these units, the average bias was estimated to be  $-0.0059$  (averaged over several points on the FTP cycle with the engine operating in steady state); the bias estimates were limited to  $-0.008 \leq \widehat{\text{bias}} \leq -0.004$ .

The initial experimental results are presented in Tables 1 through 3. The reported conversion percentage is the average of the instantaneous conversion percentages; the overall conversion percentage can be computed from the given data. The best emissions results were obtained with the full algorithm, that is, with a proportional term in the aft controller and with bias estimation enabled even during transients. The resulting emissions were consistently lower than those achieved by the baseline controller. The full algorithm achieved from 10 to 33 times less cumulative tailpipe NOx than the baseline controller, and from 1.15 to 6.2 times less cumulative tailpipe HC than the baseline controller. Figures 5 to 8 provide more details for Table 1 comparing the dual-UEGO controller of Section 3 to the baseline controller.

Figure 9 depicts a typical bias estimate throughout a portion of the FTP cycle. It is conjectured that the oscillations in the bias estimate are correlated with oscillations in the level of stored oxygen in the catalyst, which is known to promote sustained catalytic activity; see Campbell et al. (2000). The emissions results for other configurations of the controller are reported in order to confirm the “best” form of the controller and to demonstrate that the algorithm is robust in that similar results were obtained with various configurations. The most important aspect of the reported control algorithm appears to be the ability to make small adjustments the set point of the fore controller on the basis of the tailpipe  $A/F$  sensor. This is greatly facilitated by the use of a

linear sensor in the feedgas. The current algorithm exploits the linearity of the tailpipe sensor as well. Elsewhere, a version of the algorithm will be shown to function with a switching-type  $A/F$  sensor in the tailpipe position, while retaining the linear sensor for feedgas measurements.

For completeness, Table 4 presents results obtained in the final two days of testing, where the overall performance of the emissions system was significantly degraded for the baseline controller, as well as for the proposed controller. The baseline controller experienced an 80% increase in cumulative NOx, while the proposed controller underwent a ten-fold increase. Despite this, the proposed controller resulted in better NOx emissions than the baseline controller. The test cell schedule did not permit the cause of the degradation to be determined. Possible causes include: a) emissions analyzer problems; b) damage to the catalyst; and c) damage to the  $A/F$  sensors. The observations made in the time available proved that in terms of measured  $A/F$  control, the baseline controller and proposed controller performed identically to previous tests reported in Tables 1 through 3, suggesting that the  $A/F$  sensors had not changed. A purge of the emissions lines and recalibration of the emissions benches resulted in no change in reported measurements. A review of the testing log did not indicate any adverse events in the test cell that would lead to catalyst damage. Finally, impurities in the fuel seemed unlikely.

## ACKNOWLEDGMENTS

The authors sincerely thank Phil Husak, Don Lewis, Dan Meyer, and Robert Riley for their very valuable assistance, in the test cell and in numerous other ways, that led to the successful completion of this project. Deepak Aswani is thanked for his assistance in programming the real-time control computations. G. Fiengo and J.W. Grizzle gratefully acknowledge funding under a Ford Motor Company URP titled *Active Control of Aftertreatment for Improved Emissions and Fuel Economy*.

## References

- M. Ammann, H.P. Geering, C.H. Onder, C.A. Roduner, and E. Shafai. Adaptive control of a three-way catalytic converter. *American Control Conference*, 2000.
- B. Campbell, R. Farrington, G. Inman, S. Dinsdale, D. Gregory, D. Eade, and J. Kisenyi. Improved three-way catalyst performance using an active bias control regeneration system. *SAE paper 2000-01-0499*, 2000.
- A.D. Colvin, J.W. Butler, and J.E. Anderson. Catalytic effects on ZrO<sub>2</sub> oxygen sensors exposed to non-equilibrium gas mixtures. *J. Electroanal. Chem.*, (136), 1982.

- J.A. Cook, J.W. Grizzle, and J. Sun. Automotive engine control. *The Control Handbook*, CRC Press, W. Levine, pages 1261–1274, 1996.
- G. Fiengo, J.W. Grizzle, and J.A. Cook. Fore-aft oxygen storage control. *American Control Conference*, 2002.
- H. Germann, S. Tagliaferri, and H.P. Geering. Differences in pre- and post-converter lambda sensor characteristics. *SAE paper 960335*, 1996.
- H.J. Germann, C.H. Onder, and H.P. Geering. Fast gas concentration measurements for model validation of catalytic converters. *SAE paper 950477*, 1995.
- J.W. Grizzle, J.A. Cook, and W.P. Milam. Improved cylinder air charge estimation for transient air fuel ratio control. *American Control Conference*, 1994.
- D.R. Hamburg, J.A. Cook, W.J. Kaiser, and E.M. Logothetis. An engine-dynamometer study of the a/f compatibility between a three-way catalyst and an exhaust gas oxygen sensor. *SAE paper 830986*, 1983.
- E. Shafai, C. Roduner, and H.P. Geering. Indirect adaptive control of a three-way catalyst. *SAE paper 961038*, 1996.
- M.A. Shulman and D.R. Hamburg. Non-ideal properties of ZrO<sub>2</sub> and TiO<sub>2</sub> exhaust gas oxygen sensors. *SAE paper 800018*, 1980.
- A.T. Vemuri. Diagnosis of sensor bias faults. *American Control Conference*, 1999.

#### FIGURES AND TABLES OF EXPERIMENTAL DATA

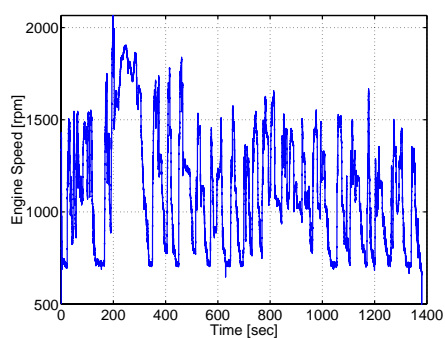


Fig. 4. Engine Speed over Test Cycle.

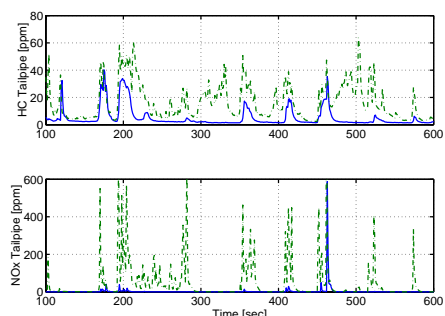


Fig. 5. Post-catalyst HC and NO<sub>x</sub> Emissions in ppm at Brick One. The solid line (blue) refers to the dual UEGO controller and the dot-dashed line (green) to the baseline controller.

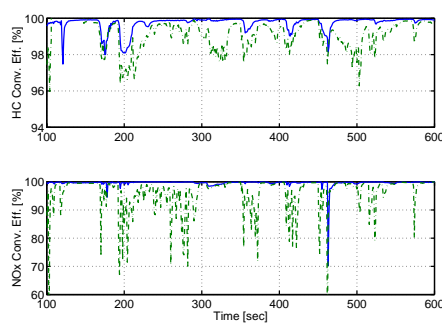


Fig. 6. Instantaneous HC and NO<sub>x</sub> Conversion Efficiencies at Brick One. The solid line (blue) refers to the dual UEGO controller and the dot-dashed line (green) to the baseline controller.

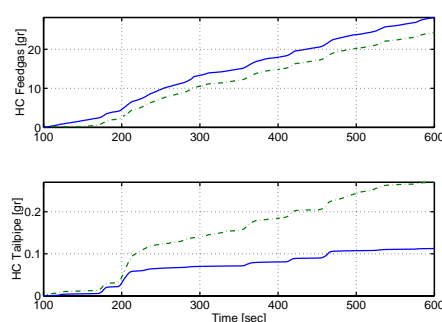


Fig. 7. Pre- and Post-catalyst Cumulative HC Emissions in Grams at Brick One. The solid line (blue) refers to the dual UEGO controller and the dot-dashed line (green) to the baseline controller.

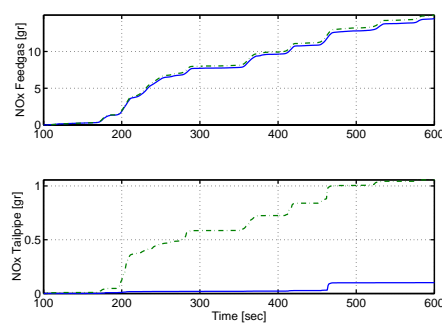


Fig. 8. Pre- and Post-catalyst Cumulative NO<sub>x</sub> Emissions in Grams at Brick One. The solid line (blue) refers to the dual UEGO controller and the dot-dashed line (green) to the baseline controller.

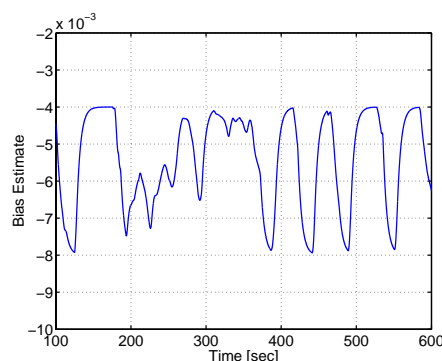


Fig. 9. Bias Estimate. Typical trace from 100 to 600 seconds when UEGO tailpipe measured at brick one.

Table 1. Emission results from 100 to 600 seconds of the FTP cycle, with tailpipe emissions collected at brick one. In a), the complete control algorithm was implemented; in b), bias estimation was used but the proportional action in the aft controller was disabled. Dual-UEGO tailpipe  $A/F$  was measured at brick one.

Controller	HC			NOx		
	Conv. eff. [%]	Tot. FG [gr]	Tot. TP [gr]	Conv. eff. [%]	Tot. FG [gr]	Tot. TP [gr]
Baseline	99.04	24.27	0.2701	93.89	14.96	1.0559
Dual UEGO <sup>a</sup>	99.76	28.15	0.1127	99.53	14.49	0.1009
Dual UEGO <sup>b</sup>	99.35	26.69	0.2071	98.80	15.06	0.2591

Table 2. Emission results from 100 to 600 seconds of the FTP cycle, with tailpipe emissions collected at brick two. In a), the complete control algorithm was implemented; in b), bias estimation was used but the proportional action in the aft controller was disabled; in c), the bias estimator was disabled during transients (see Fiengo et al. (2002)), but otherwise, the complete control algorithm was implemented. Dual-UEGO tailpipe  $A/F$  was measured at brick one for a) and at brick two for b) and c).

Controller	HC			NOx		
	Conv. eff. [%]	Tot. FG [gr]	Tot. TP [gr]	Conv. eff. [%]	Tot. FG [gr]	Tot. TP [gr]
Baseline	99.90	25.43	0.0268	98.99	17.45	0.3002
Baseline	94.57	not. av.	not.av.	97.75	not.av.	not. av.
Dual UEGO <sup>a</sup>	99.98	25.91	0.0043	99.90	14.17	0.0099
Dual UEGO <sup>a</sup>	99.92	26.91	0.0230	99.93	18.40	0.0088
Dual UEGO <sup>b</sup>	99.91	26.86	0.0311	99.72	15.45	0.0460
Dual UEGO <sup>c</sup>	99.92	24.03	0.0224	99.50	15.90	0.0805
Dual UEGO <sup>c</sup>	99.94	26.49	0.0176	99.23	16.55	0.1439
Dual UEGO <sup>c</sup>	99.89	27.72	0.0308	99.51	16.90	0.0754
Dual UEGO <sup>c</sup>	99.70	28.98	0.0926	99.61	16.62	0.0358
Dual UEGO <sup>c</sup>	99.91	28.53	0.0268	98.52	17.73	0.2258

Table 3. Emission results from 100 to 1400 seconds of the FTP cycle, with tailpipe emissions collected at brick two. In a), the complete control algorithm was implemented; in b), bias estimation was used but the proportional action in the aft controller was disabled. Dual-UEGO tailpipe  $A/F$  was measured at brick one for a) and at brick two for b).

Controller	HC			NOx		
	Conv. eff. [%]	Tot. FG [gr]	Tot. TP [gr]	Conv. eff. [%]	Tot. FG [gr]	Tot. TP [gr]
Baseline	99.91	56.69	0.0560	99.10	32.59	0.4106
Dual UEGO <sup>a</sup>	99.98	56.31	0.0091	99.89	25.55	0.0221
Dual UEGO <sup>b</sup>	99.54	not. av.	not.av.	99.55	not.av.	not. av.

Table 4. Degraded emission results obtained in final days of testing. Results are for 100 to 600 seconds of the FTP cycle, with tailpipe emissions collected at brick one. In b), bias estimation was used but the proportional action in the aft controller was disabled. Dual-UEGO tailpipe  $A/F$  was measured at brick one.

Controller	HC			NOx		
	Conv. eff. [%]	Tot. FG [gr]	Tot. TP [gr]	Conv. eff. [%]	Tot. FG [gr]	Tot. TP [gr]
Baseline	98.90	26.00	0.2887	91.54	18.57	1.8102
Dual UEGO <sup>b</sup>	98.25	26.74	0.5575	97.00	19.39	0.7158
Dual UEGO <sup>b</sup>	97.65	26.56	0.6569	95.99	18.53	1.0354